

This work was written as part of one of the author's official duties as an Employee of the United States Government and is therefore a work of the United States Government. In accordance with 17 U.S.C. 105, no copyright protection is available for such works under U.S. Law. Access to this work was provided by the University of Maryland, Baltimore County (UMBC) ScholarWorks@UMBC digital repository on the Maryland Shared Open Access (MD-SOAR) platform.

Please provide feedback

Please support the ScholarWorks@UMBC repository by emailing scholarworks-group@umbc.edu and telling us what having access to this work means to you and why it's important to you. Thank you.

Long range plasmon assisted all-optical switching at telecommunication wavelengths

Nadia Mattiucci,^{1,*} Giuseppe D'Aguanno,¹ and Mark J. Bloemer²

¹*Aegis Technologies, Nanogenesis Division, 410 Jan Davis Dr., Huntsville, Alabama 35806, USA*

²*Charles M. Bowden Laboratory, Bldg 7804, Redstone Arsenal, Alabama 35898, USA*

*Corresponding author: nadia.mattiucci@us.army.mil

Received August 15, 2011; revised November 16, 2011; accepted November 18, 2011;
posted November 18, 2011 (Doc. ID 152850); published January 6, 2012

We exploit the properties of ultranarrow, Fano-like resonances generated by the coupling of long range surface plasmons with ultrathin (~ 10 nm), metallic, subwavelength gratings embedded in a nonlinear, cubic material to obtain all-optical switching at telecommunication wavelengths for extremely low input power. We provide an example of a silver metallic grating embedded in a chalcogenide glass (As_2S_3), and we show the concrete possibility to achieve all-optical switching at local field intensities compatible with the photo-darkening threshold of the material. © 2012 Optical Society of America

OCIS Codes: 190.1450, 240.6680, 250.5403, 350.2770, 230.1150.

Long range surface plasmons (LRSPs) are guided modes excited at the surface of thin metallic layers (10 nm to 50 nm) embedded in a symmetric environment. They have been widely studied in the past both theoretically [1,2] and experimentally [3]. Because of their extremely long propagation distances and low Ohmic losses, LRSPs give rise to remarkably narrow, Lorentzian-like, attenuated total reflection (ATR) resonances in the typical prism coupling configuration [3] with bandwidths of the order of few Å. Several authors in the past have discussed the application of these narrow resonances to nonlinear optics [4] and all-optical switching in particular [5]. Besides the classical Kretschman configuration, coupling of a LRSP in a thin metal layer is also possible by patterning the metal in a periodic manner so that the LRSP can be coupled through the reciprocal lattice vector of the resulting metallic grating according to the following standard transverse momentum conservation Eqs. [6,7]:

$$k_{0,x} = |\pm k_{\text{LRSP}} \mp mG|, \quad m = 0, 1, 2, \dots \quad (1)$$

where $k_{0,x} = n_{\text{in}}k_0 \sin(\theta)$ is the transverse momentum of the incident field according to the geometry described in Fig. 1(a), n_{in} the refractive index of the incident medium, θ is the incident angle, $k_0 = 2\pi/\lambda$ the vacuum wave-vector, λ the incident wavelength, $k_{\text{LRSP}} = k_0 n_{\text{eff}}$ is the wave-vector of the LRSP, n_{eff} is the real part of the effective index of the LRSP calculated for the unperturbed (nonpatterned) metal layer as in [7], $G = 2\pi/\Lambda$ is the reciprocal lattice vector of the grating, Λ its period, and m is an integer that stands for the different diffracting orders of the grating. In [7], among other things, we have also shown that this kind of coupling gives rise to ultranarrow reflection resonances with bandwidth that can easily approach ~ 0.2 Å similar to Wood's anomalies [8]. These resonances, different from the ATR resonances, are strongly asymmetric with a typical Fano-like shape [9–11]; moreover their bandwidth is at least 1 order of magnitude narrower than the corresponding ATR resonances.

The aim of this Letter is to exploit these plasmonic Fano-resonances [7,11] for all-optical switching applica-

tions. In general, in all-optical switching devices the input intensity at the switching point scales as $1/Q^2$ [12], where $Q = \lambda/\Delta\lambda$ is the quality (Q)-factor of the resonance, so that having high- Q resonances is imperative for the purpose of a low-power all-optical switching. In our case we can readily achieve plasmonic Fano-resonances with $Q \sim 10^5$, whereas with conventional dielectric gratings, as the ones studied in [12], for example, we can have Fano-resonances with Q factors that can reach $\sim 10^4$ at most. As we pointed out in [12], increasing the Q factor beyond $\sim 10^4$ could be done by considering dielectric gratings with slit apertures well below 10 nm, which is, unfortunately, at the moment, out of reach even for the more advanced nanofabrication procedures [13]. On the contrary, as we have discussed above, ultrathin, metallic gratings naturally offer these ultranarrow, Fano-like plasmonic resonances originated by the coupling of the LRSP with the reciprocal lattice vector of the grating.

Now, let us start our analysis by describing in Fig. 1(a) the geometry we consider: a TM-polarized, monochromatic, plane wave is incident at a generic angle θ on a subwavelength, silver grating with thickness d , period Λ , and slit aperture a . The silver grating is embedded in a chalcogenide glass (As_2S_3 arsenic-trisulphide). We use chalcogenide glasses because of their large cubic nonlinearity and low two-photon absorption, two characteristics that make them ideal candidates for all-optical switching devices [14]. The dispersion of silver has been taken from the book of Palik [15] while the refractive index of As_2S_3 has been taken equal to $n_{\text{As}_2\text{S}_3} = 2.4$ in the telecommunication band (~ 1.5 – 1.6 μm) according to data reported in literature [14]. In Fig. 1(b) we show the effective index (left y -axis) n_{eff} and the propagation distance (right y -axis) as a function of λ for a LRSP propagating along a $d = 10$ nm uniform (no-grating) layer of silver embedded in As_2S_3 . We remark that the use of the bulk dispersion [15] for the 10 nm Ag layer is justified by the experimental results available in literature [16–17]. We notice that the effective index of the LRSP is very close to the refractive index of the embedding material, As_2S_3 in our case. This is a typical characteristic of LRSPs, which is due to the fact that the field of the LRSP is mostly localized in the embedding material, reducing

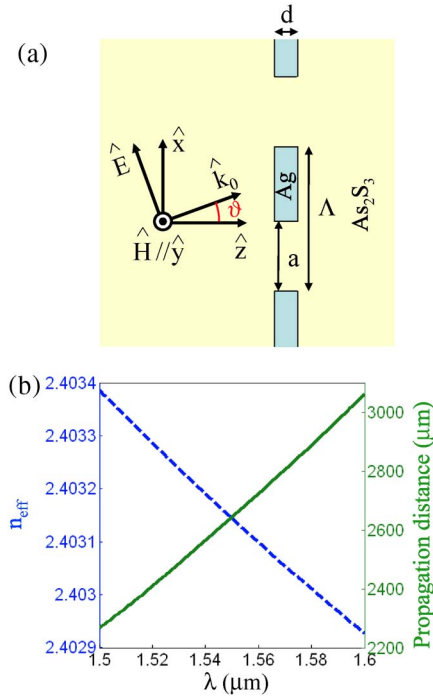


Fig. 1. (Color online) (a) Geometry: Ag grating having thickness d , period Λ and slit aperture a , embedded in As_2S_3 . We consider an electromagnetic wave, TM-polarized incident on the grating at a generic angle ϑ . (b) Effective index (left y -axis) and propagation distance (right y -axis) versus wavelength for a LRSP propagating along a 10 nm, homogeneous, Ag layer embedded in As_2S_3 .

therefore the Ohmic losses in the metal and increasing the propagation distance.

Once n_{eff} is calculated, we can use Eq. (1) to design the metallic grating for our specific needs. In our case we have chosen $\Lambda = 384$ nm to have a coupling of the LRSP with the first reciprocal lattice vector of the grating (G) in the telecommunication band for ϑ in the range between 38° and 48° , as shown in Fig. 2(a). Obviously, different frequency ranges and/or different ranges of incident angles can be explored by varying the parameters according to Eq. (1). In Fig. 2(b) we show the linear reflection (R) versus λ and ϑ for the structure described in Fig. 1(a) with the following parameters: $\Lambda = 384$ nm, $a = 240$ nm, and $d = 10$ nm. R in Fig. 2(b) has been numerically calculated using the Fourier-modal-method (FMM) [18]. In the figure it is evident the sharp variation of the reflection along the line that follows very closely the corresponding line of the coupling of the LRSP with G as predicted by Eq. (1) and shown in Fig. 2(a). There is a very slight shift between the coupling shown in Fig. 2(a) and that numerically calculated in Fig. 2(b). This is an expected phenomenon due to the fact that we have used in Eq. (1) the effective index of the LRSP of the uniform metal layer instead of the effective index of the LRSP of the metal grating.

In Fig. 3(a) we show the plasmonic Fano resonance located at $\lambda = 1.55 \mu\text{m}$ for $\vartheta = 43^\circ$. Consistent with our previous findings in the visible range [7], we note that its bandwidth is $\sim 0.2 \text{ \AA}$. On the resonance are indicated the wavelengths at which we calculate the nonlinear reflection and all-optical switching in Fig. 3(b). In the non-

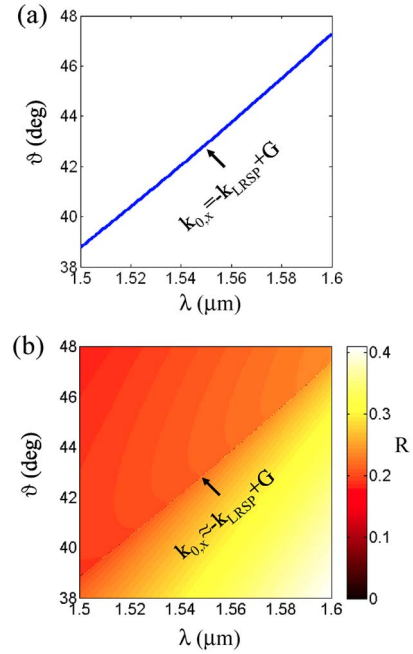


Fig. 2. (Color online) (a) Dispersion in the plane (λ, ϑ) for the LRSP coupled with the first reciprocal lattice vector of the grating with $d = 10$ nm and $\Lambda = 384$ nm. The dispersion has been calculated according to Eq. (1). (b) Reflection (R) from the structure described in Fig. 1(a) with $d = 10$ nm, $\Lambda = 384$ nm, and $a = 240$ nm.

linear case the Fano resonance undergoes considerable distortion for increasing input intensity with a typical knot-like shape in agreement with previous studies [12].

The calculation has been performed using the FMM adapted to the nonlinear case using a mean field theory similar to that proposed in [19]. The nonlinear refractive index of As_2S_3 has been taken according to [14] $n_2 = 2.9 \times 10^{-18} \text{ m}^2/\text{W}$. Switching in the range of few tens of MW/cm^2 input intensity is achievable. For example, at $\lambda = 1.5504 \mu\text{m}$ the input intensity at the switching point is $\sim 50 \text{ MW}/\text{cm}^2$. Note in particular how the switching intensity decreases if we chose λ closer to the reflection peak of the linear Fano resonance, although in this latter case lowering the input intensity is obtained at the expense of a reduction of the area of the hysteresis cycle. At the peak of reflection of the Fano resonance we have optical limiting behavior which, in this sense, corresponds to a limit hysteresis cycle with null area. At this point we would like to comment on the feasibility of our proposed device. It is well known in fact that in general chalcogenide glasses possess photo-darkening threshold for local field intensities that, for example, in the case of As_2S_3 are of the order of $\sim 1 \text{ GW}/\text{cm}^2$ [20]; therefore local field intensities not to exceed this threshold are needed for a realistic device to operate. In the following we will show that in our case the device can perform the all-optical switching under the above mentioned constraint. To this end in Fig. 3(c) for the case $\lambda = 1.5504 \mu\text{m}$ we show the field localization normalized to the incident field in the closest vicinity of the metallic grating where localization is the strongest. In particular, we have taken an observation region that starts 30 nm before the grating and ends 30 nm after the grating along the z -axis, while encompasses the entire elementary cell along the x -axis.

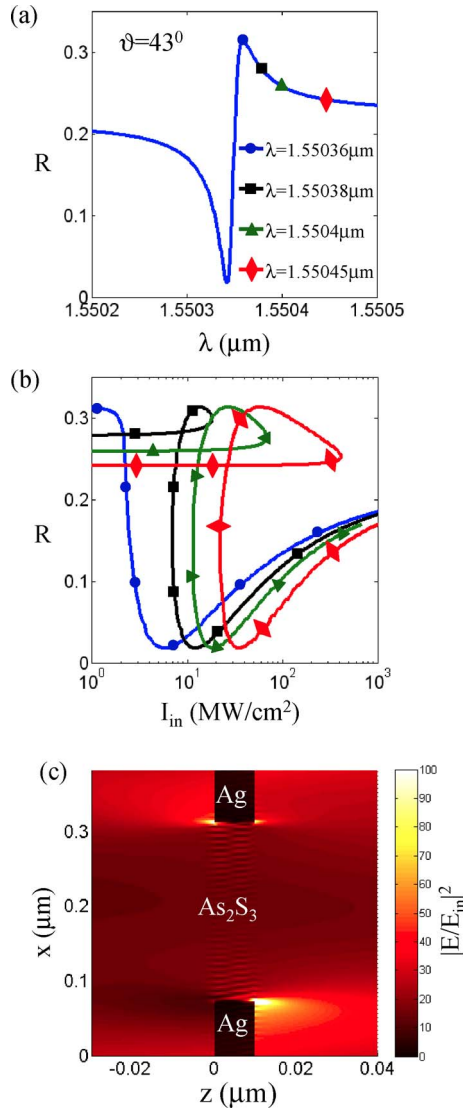


Fig. 3. (Color online) (a) Linear Fano resonance at $\lambda = 1.55 \mu\text{m}$ and $\theta = 43^\circ$. The marks on the curve indicate the operative wavelengths for the calculation reported in Fig. 3(b). (b) Nonlinear reflection versus input intensity (I_{in}) at different incident wavelengths as reported in Fig. 3(a). (c) Field localization normalized to the incident field at $\lambda = 1.5504 \mu\text{m}$ in a region very close to the metal grating as detailed in the main text.

The field is for the most part localized outside the metal, as one may expect from a LRSP, and, moreover, the average field localization in our observation region is $\langle |E/E_{\text{in}}|^2 \rangle \sim 20$, which, considering that the input intensity at the switching point is $\sim 50 \text{ MW/cm}^2$, corresponds to a local field intensity at the switching point $\sim 1 \text{ GW/cm}^2$. Although the intrinsic nonlinear response of chalcogenide glasses is ultrafast ($< 100 \text{ fs}$) [14], the exploitation of high-Q resonances may limit the possibility of an ultrafast all-optical switching because longer pulses are necessary to resolve these resonances. In our case we expect the switch to happen on a 100 ps to 1 ns time scale. In conclusion, we have shown that

plasmonic, Fano-resonances generated by the coupling of LRSPs with subwavelength, ultrathin, metallic gratings can be successfully used for all-optical switching applications in conjunction with chalcogenide glasses or any other material that possesses high cubic nonlinearity and low two-photon absorption. Moreover, although in this Letter we have given a particular example for the telecommunication band, the same concepts laid out here can apply as well to other regions of the electromagnetic spectrum such as the visible, for example. Also, apart from the self-switching based on optical bistability analyzed in this Letter, another interesting switching configuration for the same structure could be the one that involves the use of one pump laser to control the signal light.

N. M. and G. D. acknowledge financial support from Defense Advanced Research Projects Agency (DARPA) Small Business Innovation Research project Nonlinear Plasmonic Devices.

References

1. D. Sarid, Phys. Rev. Lett. **47**, 1927 (1981).
2. J. J. Burke, G. I. Stegeman, and T. Tamir, Phys. Rev. B **33**, 5186 (1986).
3. J. C. Quail, J. G. Rako, and H. J. Simon, Opt. Lett. **8**, 377 (1983).
4. G. I. Stegeman, J. J. Burke, and D. G. Hall, Appl. Phys. Lett. **41**, 906 (1982).
5. R. K. Hickernell and D. Sarid, J. Opt. Soc. Am. B **3**, 1059 (1986).
6. H. Raether, in *Springer Tracts* (Modern Physics, 1988).
7. G. D'Aguanno, N. Mattiucci, A. Alu', and M. J. Bloemer, Phys. Rev. B **83**, 035426 (2011).
8. R. W. Wood, Philos. Mag. **4**, 396 (1902).
9. U. Fano, Phys. Rev. **124**, 1866 (1961).
10. A. E. Miroshnichenko, S. Flach, and Y. S. Kivshar, Rev. Mod. Phys. **82**, 2257 (2010).
11. B. Luk'yanchuk, N. I. Zheludev, S. A. Maier, N. J. Halas, P. Nordlander, H. Giessen, and C. T. Chong, Nat. Mat. **9**, 707 (2010).
12. G. D'Aguanno, D. de Ceglia, N. Mattiucci, and M. J. Bloemer, Opt. Lett. **36**, 1984 (2011).
13. H. Duan, D. Winston, J. K. W. Yang, B. M. Cord, V. R. Manfrinato, and K. K. Berggren, J. Vac. Sci. Technol. B **28**, C6 (2010).
14. V. Ta'eed, N. J. Baker, L. Fu, K. Finsterbusch, M. R. E. Lamont, D. J. Moss, H. C. Nguyen, B. J. Eggleton, D. Y. Choi, S. Madden, and B. Luther-Davis, Opt. Express **15**, 9205 (2007).
15. E. D. Palik, *Handbook of Optical Constants of Solids* (Academic, 1991).
16. A. I. Maarouf and D. S. Sutherland, J. Phys. D **43**, 405301 (2010).
17. T. Okamoto, K. Kakutani, T. Yoshizaki, M. Haraguchi, and M. Fukui, Sur. Sci. **544**, 67 (2003).
18. G. D'Aguanno, N. Mattiucci, M. J. Bloemer, D. de Ceglia, M. A. Vincenti, and A. Alu', J. Opt. Soc. Am. B **28**, 253 (2011).
19. P. Vicent, N. Paire, M. Nevier, A. Koster, and R. Reinisch, J. Opt. Soc. Am. B **2**, 1106 (1985).
20. N. Hô, J. M. Laniel, R. Valée, and A. Villeneuve, Opt. Lett. **28**, 965 (2003).